

Observations and Mechanistic Insights on Unusual Stability of Neutral Nickel Complexes with a Sterically Crowded Metal Center

Dong-Po Song,^{†,‡,§} Yong-Xia Wang,^{†,§} Hong-Liang Mu,^{†,‡} Bai-Xiang Li,^{†,‡} and Yue-Sheng Li^{*†}[†]State Key Laboratory of Polymer Physics and Chemistry, Changchun Institute of Applied Chemistry, Chinese Academy of Sciences, Changchun 130022, People's Republic of China, and [‡]Graduate School of the Chinese Academy of Sciences, Changchun Branch, Changchun 130023, People's Republic of China

Received July 25, 2010

A series of novel nickel(II) methyl pyridine complexes based on β -ketiminato and phenoxyiminato ligands, [(2,6-¹Pr₂C₆H₃)N=CH(8-R₁C₁₀H₇)O]Ni(Me)(Py) (**5a**, R₁ = phenyl; **5b**, R₁ = norbornyl), [(2,6-¹Pr₂C₆H₃)N=CH(8-R₁C₁₀H₅)O]Ni(Me)(Py) (**6a**, R₁ = phenyl; **6b**, R₁ = norbornyl), and [(2,6-¹Pr₂C₆H₃)N=CHCHC(2'-R₂C₆H₄)O]Ni(Me)(Py) (**7a**, R₂ = H; **7b**, R₂ = phenyl), have been synthesized and characterized. Molecular structures of **5a** and **6b** were further confirmed by X-ray crystallographic analysis. These complexes showed very different catalytic properties for ethylene polymerization. Design and construction of a special catalyst structure like **5a** with a phenyl group directed toward the nickel(II) center proved to be an effective strategy for improving catalyst stability. Remarkably, according to ¹H NMR spectroscopy, bis-ligated deactivation of complex **5a** was entirely avoided, while a rapid deactivation rate was observed with regard to the parent complex **C** without a phenyl group in the R₁ position. As a result, higher activities of complex **5a** were obtained relative to complex **C** under the same polymerization conditions. In addition, the ligand backbone was found to have a great influence on polymerization behaviors. Specifically, the polyethylenes with greatly decreased molecular weights were produced by neutral nickel phenoxyiminato catalysts **6a,b** in comparison with values for the corresponding β -ketiminato catalysts **5a,b**. This is best explained by DFT results that the ethylene insertion and chain termination barriers for complex **6a** are very different from those of complex **5a**.

Introduction

Late transition metal catalysts for olefin polymerization are under intense investigation because of their unique features that are different from early transition metal systems.¹ The cationic nickel(II) and palladium(II) catalysts discovered by Brookhart and co-workers have greatly

stimulated this area.^{2–10} At the beginning of the century, Grubbs and co-workers successfully developed a series of single-component neutral nickel catalysts based on salicylaldiminato ligands that showed excellent performance in ethylene polymerization.¹¹ Compared with their cationic counterparts, these neutral catalysts are less electrophilic systems in the presence of polar monomers or solvents. This remarkably invigorated the area of neutral nickel catalysts for olefin polymerization, and a large number of such catalysts have been explored.^{12–19} For example, the nickel(II) methyl

*To whom correspondence should be addressed. Fax: +86-431-85262039. E-mail: ysli@ciac.jl.cn.

[§]These authors contributed equally to this work.

(1) (a) Ittel, S. D.; Johnson, L. K.; Brookhart, M. *Chem. Rev.* **2000**, *100*, 1169. (b) Boffa, L. S.; Novak, B. M. *Chem. Rev.* **2000**, *100*, 1479. (c) Mecking, S. *Coord. Chem. Rev.* **2000**, *203*, 325. (d) Gibson, V. C.; Spitzmesser, S. K. *Chem. Rev.* **2003**, *103*, 283. (e) Nakamura, A.; Ito, S.; Nozaki, K. *Chem. Rev.* **2009**, *109*, 5215.

(2) Johnson, L. K.; Killian, C. M.; Brookhart, M. *J. Am. Chem. Soc.* **1995**, *117*, 6414.

(3) (a) Johnson, L. K.; Mecking, S.; Brookhart, M. *J. Am. Chem. Soc.* **1996**, *118*, 267. (b) Mecking, S.; Johnson, L. K.; Wang, L.; Brookhart, M. *J. Am. Chem. Soc.* **1998**, *120*, 888. (c) Li, W.; Zhang, X.; Meetsma, A.; Hessen, B. *J. Am. Chem. Soc.* **2004**, *126*, 12246. (d) Chen, G.; Guan, Z. *J. Am. Chem. Soc.* **2004**, *126*, 2662. (e) Luo, S.; Jordan, R. F. *J. Am. Chem. Soc.* **2006**, *128*, 12072. (f) Drent, E.; van Dijk, R.; van Ginkel, R.; van Oort, B.; Pugh, R. I. *Chem. Commun.* **2002**, 744.

(4) (a) Gates, D. P.; Svejda, S. A.; Onate, E.; Killian, C. M.; Johnson, L. K.; White, P. S.; Brookhart, M. *Macromolecules* **2000**, *33*, 2320. (b) Leatherman, M. D.; Brookhart, M. *Macromolecules* **2001**, *34*, 2748.

(5) (a) Camacho, D. H.; Guan, Z. B. *Organometallics* **2005**, *24*, 4933. (b) Leung, D. H.; Guan, Z. B. *J. Am. Chem. Soc.* **2008**, *130*, 7538.

(6) (a) Burns, C. T.; Jordan, R. F. *Organometallics* **2007**, *26*, 6737. (b) Chen, C.; Luo, S.; Jordan, R. F. *J. Am. Chem. Soc.* **2008**, *27*, 12892.

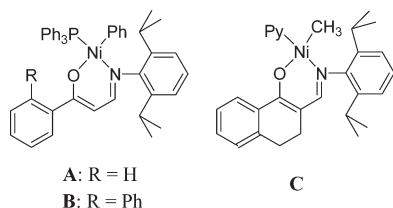
(7) (a) Speiser, F.; Braunstein, P. *Inorg. Chem.* **2004**, *43*, 1649. (b) Kermagoret, A.; Braunstein, P. *Organometallics* **2008**, *27*, 88. (c) Chavez, P.; Braunstein, P. *Organometallics* **2009**, *28*, 1776.

(8) (a) Rose, G. M.; Coates, G. W. *J. Am. Chem. Soc.* **2006**, *128*, 4186. (b) Rose, G. M.; Coates, G. W. *Macromolecules* **2008**, *41*, 9548.

(9) (a) Huang, Y. B.; Jin, G. X. *Organometallics* **2008**, *27*, 259. (b) Han, F. B.; Sun, X. L.; Tang, Y. *Organometallics* **2008**, *27*, 1924. (c) Gao, R.; Sun, W. H. *Organometallics* **2008**, *27*, 5641. (d) Brasse, M.; Campora, J. *Organometallics* **2008**, *27*, 4711. (e) Long, J. M.; Gao, H. Y.; Wu, Q. *Eur. J. Inorg. Chem.* **2008**, 4296. (f) Dorcier, A.; Basset, J. M. *Organometallics* **2009**, *28*, 2173. (g) Liu, F. S.; Gao, H. Y.; Wu, Q. *Macromolecules* **2009**, *42*, 7789. (h) Noda, S.; Nozaki, K. *Organometallics* **2009**, *28*, 656.

(10) Azoulay, J. D.; Schneider, Y.; Galland, G. B.; Bazan, G. C. *Chem. Commun.* **2009**, 6177.

Scheme 1. Neutral Nickel β -Ketiminato Complexes Reported Previously



salicylaldiminato pyridine catalysts reported by Mecking's group, bearing substituted aryls at the 2,6-positions of the N-aryl moiety, displayed high efficiency for ethylene (co)polymerization.^{12,13} Brookhart and co-workers

(11) (a) Wang, C.; Friedrich, S.; Younkin, T. R.; Li, R. T.; Grubbs, R. H.; Bansleben, D. A.; Day, M. W. *Organometallics* **1998**, *17*, 3149. (b) Younkin, T. R.; Connor, E. F.; Henderson, J. I.; Friedrich, S. K.; Grubbs, R. H.; Bansleben, D. A. *Science* **2000**, *287*, 460. (c) Connor, E. F.; Younkin, T. R.; Henderson, J. I.; Hwang, S.; Grubbs, R. H.; Roberts, W. P.; Litzau, J. J. *J. Polym. Sci., Polym. Chem. Ed.* **2002**, *40*, 2842. (d) Connor, E. F.; Younkin, T. R.; Henderson, J. I.; Waltman, A. W.; Grubbs, R. H. *Chem. Commun.* **2003**, 2272. (e) Guironnet, D.; Younkin, T. R.; Grubbs, R. H. *Organometallics* **2004**, *23*, 5121.

(12) (a) Zuideveld, M.; Wehrmann, P.; Röhr, C.; Mecking, S. *Angew. Chem., Int. Ed.* **2004**, *43*, 869. (b) Kuhn, P.; Sémeril, D.; Jeunesse, C.; Matt, D.; Neuburger, M.; Mota, A. *Chem.—Eur. J.* **2006**, *12*, 5210. (c) Göttker-Schnetmann, I.; Wehrmann, P.; Röhr, C.; Mecking, S. *Organometallics* **2007**, *26*, 2348. (d) Bastero, A.; Göttker-Schnetmann, I.; Röhr, C.; Mecking, S. *Adv. Synth. Catal.* **2007**, *349*, 2307. (e) Guironnet, D.; Mecking, S. *Chem. Commun.* **2008**, 4965. (f) Berkefeld, A.; Mecking, S. *J. Am. Chem. Soc.* **2009**, *131*, 1565.

(13) (a) Held, A.; Bauers, F. M.; Mecking, S. *Chem. Commun.* **2000**, 301. (b) Bauers, F. M.; Mecking, S. *Macromolecules* **2001**, *34*, 1165. (c) Bauers, F. M.; Mecking, S. *Angew. Chem., Int. Ed.* **2001**, *40*, 3020. (d) Bauers, F. M.; Chowdhry, M. M.; Mecking, S. *Macromolecules* **2003**, *36*, 6711. (e) Bauers, F. M.; Thomann, R.; Mecking, S. *J. Am. Chem. Soc.* **2003**, *125*, 8838. (f) Kolb, L.; Monteil, V.; Thomann, R.; Mecking, S. *Angew. Chem., Int. Ed.* **2005**, *44*, 429–432. (g) Wehrmann, P.; Mecking, S. *Macromolecules* **2006**, *39*, 5963. (h) Wehrmann, P.; Zuideveld, M. A.; Thomann, R.; Mecking, S. *Macromolecules* **2006**, *39*, 5995. (i) Göttker-Schnetmann, I.; Korthals, B.; Mecking, S. *J. Am. Chem. Soc.* **2006**, *128*, 7708. (j) Weber, C. H. M.; Chiche, A.; Krausch, G.; Rosenfeldt, S.; Ballauf, M.; Harnau, L.; Göttker-Schnetmann, I.; Tong, Q.; Mecking, S. *Nano Lett.* **2007**, *7*, 2024.

(14) (a) Hicks, F. A.; Brookhart, M. *Organometallics* **2001**, *20*, 3217. (b) Jenkins, J. C.; Brookhart, M. *Organometallics* **2003**, *22*, 250. (c) Hicks, F. A.; Jenkins, J. C.; Brookhart, M. *Organometallics* **2003**, *22*, 3533. (d) Jenkins, J. C.; Brookhart, M. *J. Am. Chem. Soc.* **2004**, *126*, 5827.

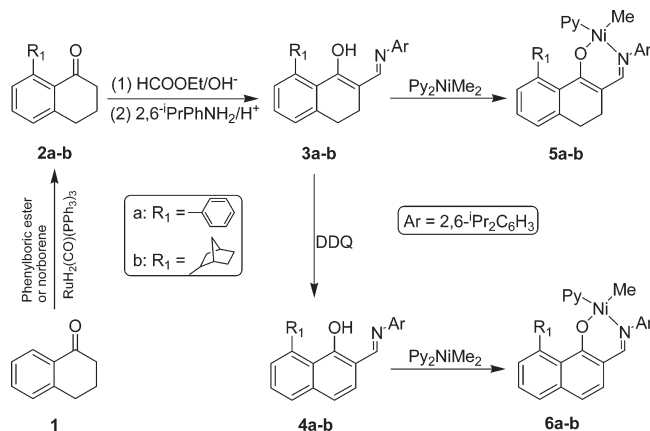
(15) (a) Soula, R.; Broyer, J. P.; Llauro, M. F.; Tomov, A.; Spitz, R.; Claverie, J.; Drujon, X.; Malinge, J.; Saudemont, T. *Macromolecules* **2001**, *34*, 2438. (b) Gibson, V. C.; Tomov, A.; White, A. J. P.; Williams, D. J. *Chem. Commun.* **2001**, 719. (c) Tian, G. L.; Boone, H. W.; Novak, B. M. *Macromolecules* **2001**, *34*, 7656. (d) Li, X. F.; Li, Y. S. *J. Polym. Sci., Part A: Polym. Chem.* **2002**, *40*, 2680. (e) Li, Y. S.; Li, Y. R.; Li, X. F. *J. Organomet. Chem.* **2003**, 667. (f) Zhang, D.; Jing, G. X. *Organometallics* **2003**, *22*, 2851. (g) Liang, H.; Liu, J. Y.; Li, X. F.; Li, Y. S. *Polyhedron* **2004**, *23*, 1619. (h) Zhang, D.; Jin, G.-X. *Inorg. Chem. Commun.* **2006**, *9*, 1322.

(16) (a) Sujith, S.; Dae, J. J.; Na, S. J.; Park, Y.-W.; Choi, J. H.; Lee, B. Y. *Macromolecules* **2005**, *38*, 10027. (b) Na, S. J.; Lee, B. Y. *J. Organomet. Chem.* **2006**, *691*, 611. (c) Zeller, A.; Strassner, T. *J. Organomet. Chem.* **2006**, *691*, 4379. (d) Okada, M.; Shiono, T. *J. Organomet. Chem.* **2007**, *692*, 5183. (e) Chen, Q.; Yu, J.; Huang, J. *Organometallics* **2007**, *26*, 617. (f) Wei, W. P.; Huang, B. T. *Inorg. Chem. Commun.* **2008**, *11*, 487. (g) Shen, M.; Sun, W. H. *J. Organomet. Chem.* **2008**, *693*, 1683. (h) Li, W. F.; Sun, H. M.; Shen, Q. *J. Organomet. Chem.* **2008**, *693*, 2047. (i) Chandran, D.; Kim, I. *J. Organomet. Chem.* **2009**, *694*, 1254.

(17) (a) Hu, T.; Tang, L. M.; Li, X. F.; Li, Y. S.; Hu, N. H. *Organometallics* **2005**, *24*, 2628. (b) Rodriguez, B. A.; Delferro, M.; Marks, T. J. *Organometallics* **2008**, *27*, 2166. (c) Rodriguez, B. A.; Delferro, M.; Marks, T. J. *J. Am. Chem. Soc.* **2009**, *131*, 5902.

(18) (a) Zhang, L.; Brookhart, M.; White, P. S. *Organometallics* **2006**, *25*, 1868. (b) Yu, S. M.; Mecking, S.; et al. *Macromolecules* **2007**, *40*, 421.

Scheme 2. General Synthetic Route of the Neutral Nickel Complexes 5a,b and 6a,b

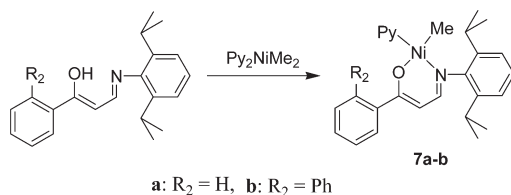


demonstrated that neutral nickel catalysts containing five-membered nickel chelates exhibited high activities toward ethylene polymerization.¹⁴ The mechanistic investigations of these neutral nickel catalysts provided us detailed information about the catalytic process.^{12f,14d}

With regard to the neutral nickel salicylaldiminato complex, a bulky substituent at the ortho position of the phenoxy group is necessary to enhance the catalytic activity by accelerating triphenylphosphine dissociation and decreasing the rate of catalyst deactivation. In our recent report, a series of modified neutral nickel β -ketoiminato catalysts were found to be highly active toward ethylene polymerization.^{19b} As shown in Scheme 1, the phenyl-substituted catalyst **B** exhibited a higher activity relative to the parent catalyst **A**, because the phenyl group can promote catalyst activation and protect active species from bis-ligated deactivation when it is located at a position close to the metal center. However, such protection disappears when the phenyl group turns away from the metal center. Consequently, finding a new methodology to maintain the sterically crowded nickel center is a very interesting goal. Our recent discovery of a family of highly active nickel catalysts characterized by a cyclic β -ketiminato skeleton provides a pathway to achieve this.^{19c} In this report, complexes **5a,b** with substituents directed toward the nickel centers (Scheme 2) have been successfully prepared from complex **C** (Scheme 1). Interestingly, complex **5a** displayed an unusual stability in ethylene polymerization, and the bis-ligated deactivation of the complex was completely avoided under the polymerization conditions, which supplies a new strategy for improving the stability of the neutral nickel system. Furthermore, for a detailed investigation of different catalyst backbones, β -ketiminato complexes **7a,b** and phenoxyiminato complexes **6a,b** together with their much different ethylene polymerization behaviors are also included in this report. Further mechanistic studies revealed the different catalytic processes of the varied structures on the basis of NMR monitoring and DFT methods. Dissimilar ethylene polymerization processes of complexes **C** and **5a** have been directly observed by ¹H NMR spectroscopy at room temperature.

(19) (a) Li, X. F.; Li, Y. G.; Li, Y. S.; Chen, Y. X.; Hu, N. H. *Organometallics* **2005**, *24*, 2502. (b) Song, D. P.; Ye, W. P.; Wang, Y. X.; Liu, J. Y.; Li, Y. S. *Organometallics* **2009**, *28*, 5697. (c) Song, D. P.; Wu, J. Q.; Ye, W. P.; Mu, H. L.; Li, Y. S. *Organometallics* **2010**, *29*, 2306.

Scheme 3. General Synthetic Route of the Neutral Nickel Complexes 7a,b



Results and Discussion

Synthesis and Characterization of the Neutral Nickel Complexes.

A general synthetic route for the neutral nickel complexes **5a,b** and **6a,b** used in this study is shown in Scheme 2. Substituted 1-tetralones **2a,b** were prepared via the reaction between 1-tetralone, phenylboric acid, and norbornene, respectively, with RuH₂(CO)(PPh₃)₃ as a catalyst. β-Diketones were first prepared via the reaction between ethyl formate and the corresponding substituted 1-tetralones, with the help of a strong base, such as potassium *tert*-butoxide, in anhydrous diethyl ether. β-Ketiminates **3a,b** were prepared in good yields by the condensation of the corresponding β-diketones with 2,6-diisopropylaniline in ethanol containing a small amount of formic acid as a catalyst. Ligands **4a,b** were obtained from compounds **3a,b** using 2,3-dichloro-5,6-dicyanobenzoquinone (DDQ) as the oxidant. According to the literature,^{12c} nickel methyl pyridine complexes **5a,b**, **6a,b**, and **7a,b** were prepared in high yields by adding (pyridine)₂NiMe₂ to the toluene solutions of their ligands with vigorous stirring at room temperature for about 4 h (see Schemes 2 and 3).

The neutral nickel complexes **5a,b**, **7a,b**, and **6a,b**, bearing β-ketiminato and phenoxyiminato ligands, are clearly characterized by ¹H and ¹³C NMR spectra. To further confirm the structures of these complexes, crystals of **5a** and **6b** suitable for X-ray crystallographic analysis were grown from hexane solutions. The data collection and refinement data of the analysis are summarized in Table S1 (see Supporting Information), and the ORTEP diagrams are shown in Figures 1 and 2 together with selected bond distances and angles, respectively. In the solid state, both of the complexes adopt a near-square-planar coordination geometry, and the pyridine group is *trans* to the N-aryl group just like the nickel methyl pyridine complexes reported previously by Mecking's group.^{12a} However, there are also some differences between complexes **5a** and **6b**. An intriguing difference is that they have different molecular backbones, which can be described as soft and rigid structures. Complex **5a** displays a torsion angle of C9–C10–C1–O (30.67°) much larger than that of complex **6b** (9.34°). In addition, complex **6b** exhibits relatively longer O–C1, C1–C2, and C2–C11 bond distances than those of complex **5a** due to an enhanced degree of conjugation. Another difference is that **6b** shows a Ni–C bond distance (1.928(4) Å) apparently shorter than that of **5a** (1.946(2) Å), indicating that the ligand backbone may have a great influence on the electronic environment of the nickel center.

There is no visible difference in Ni–X bond distances between **6b** and the other phenoxyiminato nickel methyl pyridine complexes.^{12a} However, the C–O bond and its phenyl ring are distorted because of the steric hindrance derived from a bulky norbornyl group. The steric interaction has been also confirmed by the similar torsion of the

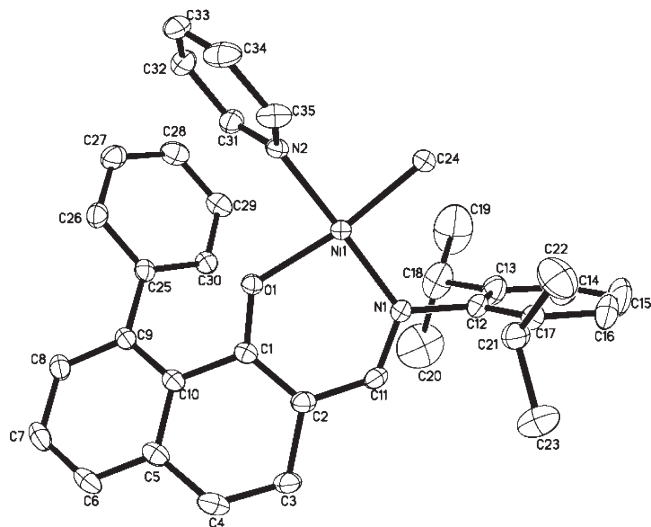


Figure 1. Molecular structure of complex **5a**. Thermal ellipsoids are drawn at the 30% probability level, and H atoms are omitted for clarity. Selected bond distances (Å) and angles (deg): Ni–C(24) = 1.946(2), Ni–N(1) = 1.8825(15), Ni–O = 1.9157(12), Ni–N(2) = 1.9119(15), O–C(1) = 1.283(2), N(1)–C(11) = 1.316(2), N(1)–C(12) = 1.447(2), C(1)–C(2) = 1.387(3), C(2)–C(11) = 1.396(3), N(1)–Ni–N(2) = 175.50(7), O–Ni–C(24) = 171.07(8), O–Ni–N(2) = 85.55(6), O–Ni–N(1) = 93.51(6), C(24)–Ni–N(1) = 93.77(8), C(24)–Ni–N(2) = 87.58(8).

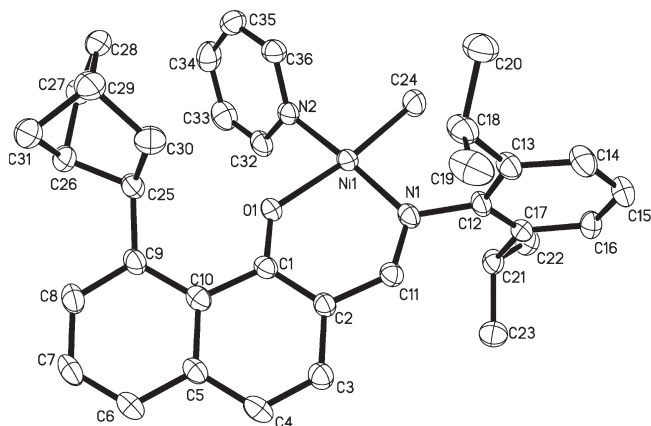


Figure 2. Molecular structure of complex **6b**. Thermal ellipsoids are drawn at the 30% probability level, and H atoms together with half of a hexane molecule are omitted for clarity. Selected bond distances (Å) and angles (deg): Ni–C(24) = 1.928(4), Ni–N(1) = 1.884(3), Ni–O = 1.915(2), Ni–N(2) = 1.912(3), O–C(1) = 1.291(4), N(1)–C(11) = 1.307(4), N(1)–C(12) = 1.448(4), C(1)–C(2) = 1.404(5), C(2)–C(11) = 1.429(5), N(1)–Ni–N(2) = 174.21(13), O–Ni–C(24) = 172.97(14), O–Ni–N(2) = 85.11(11), O–Ni–N(1) = 93.88(11), C(24)–Ni–N(1) = 92.62(15), C(24)–Ni–N(2) = 88.67(15).

C9–C25 bond and its phenyl group in the opposite direction. For instance, the torsion angle of O–C1–C10–C5 is about 11.3°, while the torsion angle of C25–C9–C10–C5 is about –5.9° (minus represents the opposite direction).

Ethylene Polymerization Based on β-Ketiminato Neutral Nickel Catalysts. The neutral nickel β-ketiminato complexes **5a,b** and **7a,b** were investigated as the catalysts for ethylene polymerization in toluene under or without the help of

Table 1. Results of Ethylene Polymerization Reactions^a

entry	complex (μmol)	T ($^{\circ}\text{C}$)	polymer (g)	activity ^b	T_m ($^{\circ}\text{C}$)	M_w ^c (kg/mol)	M_w/M_n ^c	branches ^d /1000C
1-1	5a (10)	63	7.7	46	99	21.9	2.2	39
1-2 ^e	5a (10)	63	5.0	30	97	18.2	1.9	51
1-3 ^f	5a (10)	73	5.7	68	91	9.40	2.0	60
1-4	5b (20)	63	1.9	5.7	94	15.8	2.1	65
1-5 ^f	5b (20)	63	0.6	3.6	— ^h	8.29	1.8	76
1-6 ^g	6a (10)	59–82	7.0	42	93	1.20	1.6	46
1–7	6a (10)	53	1.9	11	101	2.04	1.7	40
1-8	6a (10)	63	5.9	35	97	1.60	1.6	44
1-9	6a (10)	73	6.0	36	90	1.33	1.6	57
1-10 ^g	6b (10)	50	1.1	6.6	89	3.06	1.8	49
1-11	6b (10)	63	2.5	15	— ^h	2.24	1.6	71
1-12 ^f	7a (20)	63	5.2	31	99	23.9	2.1	35
1-13 ^f	7b (20)	63	6.4	38	94	19.0	1.9	41

^a Reaction conditions: 100 mL of toluene, 2 equiv of $\text{B}(\text{C}_6\text{F}_5)_3$ (B/Ni = 2), ethylene pressure of 50 atm, polymerization for 20 min. ^b In units of kg of PE/((mol of Ni) h atm). ^c Determined by GPC. ^d Calculated from ^1H NMR. ^e Equiv of $\text{B}(\text{C}_6\text{F}_5)_3$ (B/Ni = 1) added. ^f Ethylene pressure is 25 atm. ^g Polymerization in 60 mL of toluene. ^h Completely amorphous polymer.

Table 2. Ethylene Polymerization with **c, **5a**, and **7a,b** in the Presence of Pyridine^a**

entry	catalyst	T ($^{\circ}\text{C}$)	polymer (g)	activity ^b	T_m ($^{\circ}\text{C}$)	M_w ^c (kg/mol)	M_w/M_n ^c
2-1 ^d	C	63	3.5	21	98	38.6	2.0
2-2	C + 5 equiv of Py	63	trace				
2-3	5a	63	10.2	61	88	15.3	1.9
2-4	5a + 5 equiv of Py	63	3.0	18	91	13.3	1.9
2-5	7a	63	4.7	28	99	24.0	2.1
2-6	7a + 5 equiv of Py	63	trace				
2-7	7b	63	4.9	29	91	17.1	1.9
2-8	7b + 5 equiv of Py	63	1.4	8.4	— ^e	17.3	1.9

^a Reaction conditions: 20 μg catalyst in 100 mL of toluene, ethylene pressure of 25 atm, polymerization for 20 min. ^b In units of kg of PE/((mol of Ni) h atm). ^c Determined by GPC. ^d Reported in the literature. ^e Completely amorphous polymer.

$\text{B}(\text{C}_6\text{F}_5)_3$. The typical results are summarized in Tables 1 and 2. The data in the tables indicate that a substituent greatly influences catalytic activity and polymer microstructure along with properties. Complex **5a** was prepared by introducing a phenyl group in the R_1 position of complex **C** to explore the steric effect on ethylene polymerization behavior. Interestingly, a visible increase of activity (catalyst **5a**) was observed in comparison to catalyst **C** under the same conditions (63 $^{\circ}\text{C}$, ethylene pressure of 50 or 25 atm). Activated by $\text{B}(\text{C}_6\text{F}_5)_3$, catalyst **5a** showed a higher activity of 46 kg of PE/((mol of Ni) h atm) (entry 1-1) relative to the parent catalyst **C** (36 kg of PE/((mol of Ni) h atm)).^{19c} Used as a single-component catalyst, **5a** displayed a significantly increased activity (51 kg of PE/((mol of Ni) h atm), entry 2-3) in comparison with that of **C** (21 kg of PE/((mol of Ni) h atm), entry 2-1).^{19c} The great influences on catalytic processes caused by the substituted phenyl group should be responsible for these differences according to subsequent mechanistic studies (vide infra).

The influence of reaction temperature on the activities of catalysts **C** and **5a** was investigated to explore the substituent effect. As shown in Figure 3, reaction temperature shows a negligible influence on activities of catalyst **5a** but not **C**. A high activity of catalyst **C** was observed only when the temperature increased to 63 $^{\circ}\text{C}$, while catalyst **5a** exhibited similar activities less dependent on temperature. As shown in Figure 4, reaction temperature displays limited influence on the molecular weights of the polyethylenes produced by catalysts **C** and **5a**. The ligand should be the major factor determining the relationship between chain propagation rate and chain walking rate, which will decide the molecular weight of the obtained polymer. In addition, polymerization reactions at 63 $^{\circ}\text{C}$ have been carried out for different times,

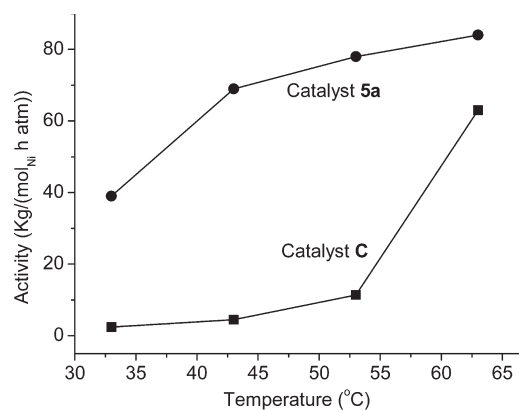


Figure 3. Influence of reaction temperature on activity. Reaction conditions: 20 μg of catalyst and 2 equiv of $\text{B}(\text{C}_6\text{F}_5)_3$ (B/Ni molar ratio = 2) in 100 mL of toluene, 25 atm of ethylene pressure, polymerization for 20 min.

such as 10, 20, 30, and 40 min, to verify catalyst deactivation. As shown in Figure 5, no deactivation of catalyst **5a** was observed within 40 min. In contrast, an obvious deactivation of catalyst **C** was detected under the same polymerization conditions. This is consistent with the results obtained from ^1H NMR observations (see Figures 7, 8, and S2).

Complexes **7a,b** were also synthesized for comparison (shown in Scheme 3). Activated by $\text{B}(\text{C}_6\text{F}_5)_3$, catalyst **7b** showed a higher activity of 38 kg of PE/((mol of Ni) h atm) (entry 1-13) relative to that of its parent catalyst **7a** (31 kg of PE/((mol of Ni) h atm), entry 1-12). Without any cocatalyst, **7a** and **7b** displayed similar activities of 28 and 29 kg of PE/((mol of Ni) h atm) (entries 2-5 and 2-7), respectively.

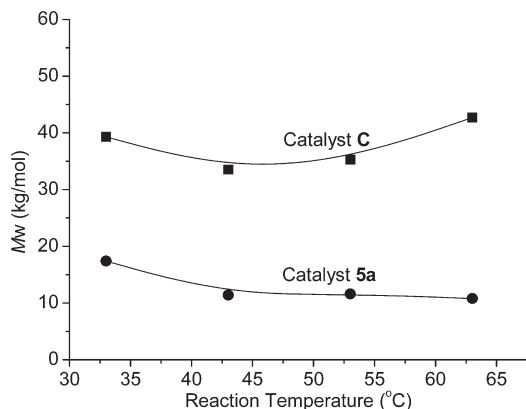


Figure 4. Influence of reaction temperature on molecular weight of polyethylene. Reaction conditions: 20 μg of catalyst and 2 equiv of $\text{B}(\text{C}_6\text{F}_5)_3$ (B/Ni molar ratio = 2) in 100 mL of toluene, 25 atm of ethylene pressure, polymerization for 20 min.

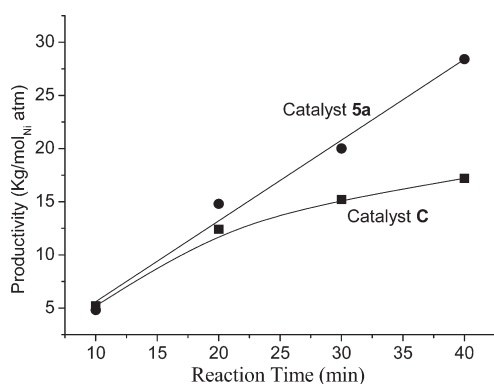


Figure 5. Productivity vs reaction time for catalysts C and 5a. Reaction conditions: 10 μg of catalyst and 2 equiv of $\text{B}(\text{C}_6\text{F}_5)_3$ (B/Ni molar ratio = 2) in 50 mL of toluene, 25 atm of ethylene pressure.

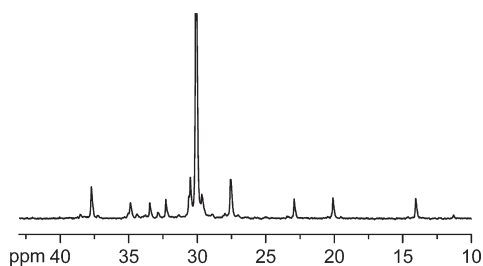


Figure 6. ^{13}C NMR of the polyethylene produced by catalyst 6a (entry 1-8).

Different from the case of catalyst 5a, the substituted phenyl group of catalyst 7b exhibits little influences on the activity due to the differences in ligand structure between the two complexes. As shown in Scheme 4, the substituted group of complex 7b can depart from the position proximate to the nickel center by free-rotating, while for structure 5a such rotating is constrained.

To further investigate the different performances of these catalysts, extra pyridine was added in catalytic systems during the ethylene polymerization process. The data listed in Table 2 indicate that complexes C and 7a without a substituent display only limited tolerance to the additional

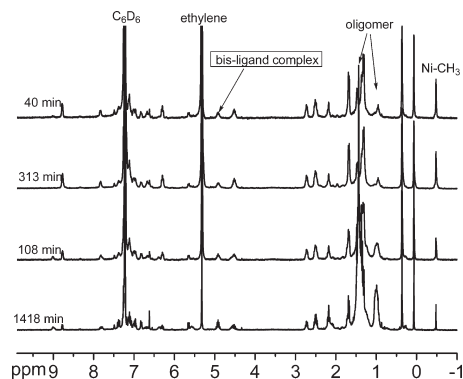


Figure 7. ^1H NMR observations of the ethylene polymerization process of catalyst C.

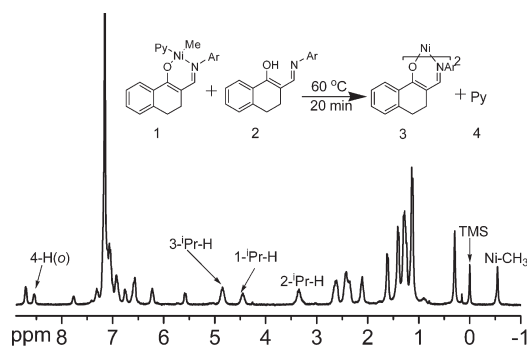
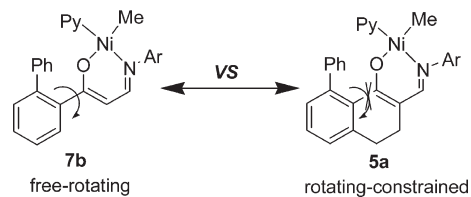


Figure 8. ^1H NMR observations of bis-ligand complex formation with catalyst C.

Scheme 4. Comparison of Structures 7b and 5a



pyridine, and very small amounts of polymers were obtained at the end of polymerization in the presence of 5 equiv of pyridine (entries 2-2 and 2-6). In contrast, catalytic properties were greatly improved by introducing a phenyl group proximate to the O atom. Complexes 5a and 7b still showed moderate activities (18 and 8.4 kg of PE/(mol of Ni) h atm, entries 2-4 and 2-8) under the same conditions. As we know, with regard to the polymerization reaction, there is an equilibrium between “Ni-ethylene” and “Ni-Py” species, and the latter is a kind of “resting state” that cannot serve for chain propagation. Ethylene molecules are much smaller than pyridine molecules. On the other hand, an ethylene molecule has a coordinating ability weaker than pyridine. Complexes 5a and 7b bearing the more bulky ligands showed visible activities when extra pyridine was added. The probable reason is that the bulky ligands can cause more hindrance to pyridine than to the smaller ethylene. Consequently, to some extent the equilibrium will be turned to the “Ni-ethylene” side where the chain propagation takes place.

Complex 5b, with a norbornyl group in the R_1 position, was also prepared and used as the catalyst for ethylene

polymerization. As shown in Table 1, catalyst **5b** displayed an activity of 5.7 kg of PE/((mol of Ni) h atm) (entry 1-4) lower than that of **5a** under the same conditions. The substituted norbornyl group caused a decrease of the activity, which seems difficult to understand. The probable reason may be that the norbornyl is more bulky than a phenyl group, leading to a larger hindrance to the chain propagation process. This is similar to the subsequent DFT calculations that show complex **5a** to exhibit an energy barrier of ethylene insertion reaction higher than that of complex **C**.

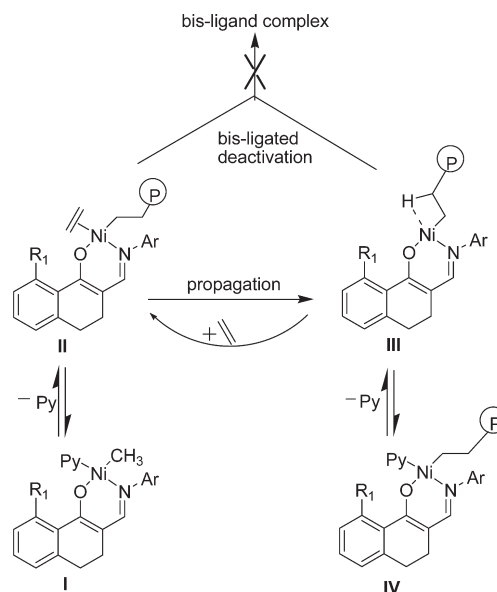
The data given in Tables 1 and 2 also indicate that the ligand structure considerably affects the molecular weight and microstructure of polyethylene obtained. In the presence of $B(C_6F_5)_3$, the weight-average molecular weights (M_w) of the polymers produced by **7a** and **7b** decrease from 23.9 to 19.0 kg/mol, while the branching numbers increase from about 35 to 41 branches per 1000 carbon atoms (entries 1-12 and 1-13). The same tendency (see entries 2-5 and 2-7) was also observed when **7a** and **7b** were used as the single-component catalysts. Analogously, polyethylene with a much lower molecular weight of 15.3 kg/mol was obtained using catalyst **5a** (entry 2-3) relative to its parent catalyst **C** (38.6 kg/mol, entry 2-1). As shown in Table 1, polyethylene with a lower molecular weight of 15.8 kg/mol (entry 1-4) was produced by catalyst **5b** in comparison to catalyst **5a** (21.9 kg/mol, entry 1-1) under the same conditions.

Ethylene pressure also dramatically affects the molecular weight and microstructure of the resulting polymers. It is noteworthy that polyethylene with much lower molecular weight can be obtained by changing pressure from 50 to 25 atm (from 15.8 to 8.29 kg/mol, entries 1-4 and 1-5) at 63 °C using catalyst **5b**. In contrast, the branching number increases with the decrease of ethylene pressure (from 65 to 76 branches/1000C, entries 1-4 and 1-5). The probable reason is that ethylene insertion is slower relative to "chain walking" under a lower ethylene concentration.

Ethylene Polymerization Based on Phenoxyiminato Neutral Nickel Catalysts. Complexes **6a,b** were also synthesized to explore the different performances between the phenoxyiminato and β -ketiminato neutral nickel catalysts. As shown in Table 1, catalyst **6a** displayed a lower activity of 35 kg of PE/((mol of Ni) h atm) (entry 1-8) relative to that of **5a** (46 kg of PE/((mol of Ni) h atm)) (entry 1-1) under the same conditions, and a polyethylene with a much lower molecular weight (1.60 kg/mol) and higher branch content (44 branches/1000C) was obtained. A completely conjugated structure of catalyst **6a** may be responsible for this, which is consistent with our previous report.^{19c} Analogously, compared with **5b**, catalyst **6b** produced polyethylenes with much lower molecular weights and higher branch contents (see entries 1-4 and 1-11). All the results have been rationalized by further DFT studies on ethylene insertion and chain termination processes (vide infra).

The influence of reaction temperature on ethylene polymerization was also investigated. As shown in Table 1, complex **6a** was chosen as the candidate for the temperature experiment. The catalytic activity was greatly enhanced from 11 kg of PE/((mol of Ni) h atm) (entry 1-7) to 36 kg of PE/((mol of Ni) h atm) (entry 1-9) by elevating the reaction temperature from 53 to 73 °C. The molecular weights of the polyethylenes decreased from 2.04 to 1.33 kg/mol, and the branch content was enhanced from 40 to 57 branches per 1000 carbon atoms, which is consistent with the reported

Scheme 5. Proposed Substituent Effect in the Polymerization Process

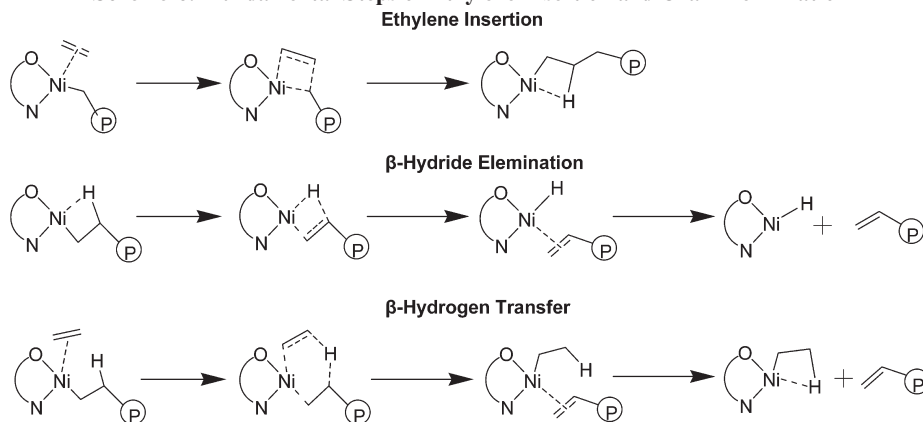


cationic nickel α -diimine catalysts as well as the neutral nickel salicylaldiminato systems.^{2,11a}

The microstructure of the typical polymer produced by catalysts **6a,b** was investigated by high-temperature 1H NMR (Figure S1) and ^{13}C NMR data (Figure 6), which indicate that methyl branches are the predominant branching style in the polymer. Interestingly, the terminal and inner double bonds are all observed from the 1H NMR data, and the inner ones are the main double bonds in the polymer chains. This suggests that a rapid chain walking reaction exists in the ethylene polymerization of the catalyst.

1H NMR Observations of Ethylene Polymerization Process. As shown in Scheme 5, the substituents may lead to a great effect on the ethylene polymerization process, which has been confirmed by subsequent NMR and DFT methods. The direct observations of the chain-growing processes of catalysts **C** and **5a** have been achieved by 1H NMR monitoring, respectively. For each experiment, an NMR tube was charged with the neutral nickel catalyst and about 0.5 mL of C_6D_6 , and then ethylene was guided into the tube for about 30 min at room temperature. Subsequently, the resulting mixture was used for 1H NMR data collection after different time periods, and the data are shown in Figure 7, from which we can see a clear ethylene polymerization process of catalyst **C**. With passing time, the signal at 5.25 ppm belonging to the ethylene monomer together with the Ni- CH_3 signal at -0.55 ppm become lower and lower, while higher and higher peaks at about 1.36 and 0.91 ppm belonging to ethylene oligomer are observed. Additionally, a rapid bis-ligated deactivation was detected, characterized by the appearance of the multiple peak at 4.85 ppm, which is assigned to the isopropyl of the bis-ligand complex (vide infra). According to Figure 7, about 38% of catalyst **C** was transformed into the bis-ligated complex after 40 min and about 52% for a period of 23.6 h. Analogously, an ethylene consumption process of catalyst **5a** is shown in Figure S2 (see Supporting Information). However, absolutely no bis-ligand complex was detected with regard to catalyst **5a** because of its sterically crowded nickel center (see Scheme 5).

Scheme 6. Fundamental Steps of Ethylene Insertion and Chain Termination



Investigations of Bis-ligated Deactivation. As we know, formation of a bis-ligated complex is the major deactivation route for the neutral nickel catalysts.^{11d,12f} Aspects of the bis-ligated deactivation are further studied in this part. A bis-ligand complex of the cyclic ligand without a substituent was successfully prepared, but the same attempt to synthesize a bis-ligand complex of **3a** was a complete failure due to the steric hindrance caused by the substituent. Bis-ligand complex formation with catalysts **C** and **5a** was investigated by ¹H NMR spectroscopy. For each experiment, an NMR tube was charged with the neutral nickel complex (single-ligand complex) and the corresponding ligand precursor in a molar ratio of about 0.7:1 in 0.5 mL of C₆D₆. Then the NMR tube was heated to 60 °C for 20 min and then used for ¹H NMR data collection. As shown in Figure 8, formation of the bis-ligand complex of the cyclic ligand without a substituent was observed by ¹H NMR spectroscopy, and about 44% of catalyst **C** was transformed into the bis-ligated complex. In contrast, no such bis-ligated deactivation of phenyl-substituted catalyst **5a** was detected under the same conditions (see Figure S3 in the Supporting Information), because the phenyl group can efficiently hinder the protonolysis of the Ni-alkyl moiety with the ligand precursor. This is in line with the reports that bulky substituted salicylaldiminato ligands hinder catalyst decomposition.^{11,12f} In our previous report, complex **B** showed a lower bis-ligated deactivation rate relative to the parent complex **A**, but the formation of a bis-ligand complex was not fully prevented.^{19b} Here, such a deactivation pathway was entirely blocked because of the sterically crowded nickel center of complex **5a** (see Scheme 5) under the reaction conditions.

DFT Studies of Ethylene Insertion and Chain Termination Reactions. There is a competitive relationship between the ethylene insertion reaction and the chain termination reaction, which determines the molecular weight of the polyethylene produced.^{21a} In order to find the correlation of the reactions with catalyst structure, DFT investigations were employed for both ethylene insertion reaction and chain termination reaction of catalysts **C**, **5a**, and **6a**. As shown in Scheme 6, two major chain termination reactions, β-hydride elimination (BHE) and β-hydrogen transfer (BHT), were investigated in this paper. The BHE and BHT energy profiles were evaluated by linear transit method with chosen

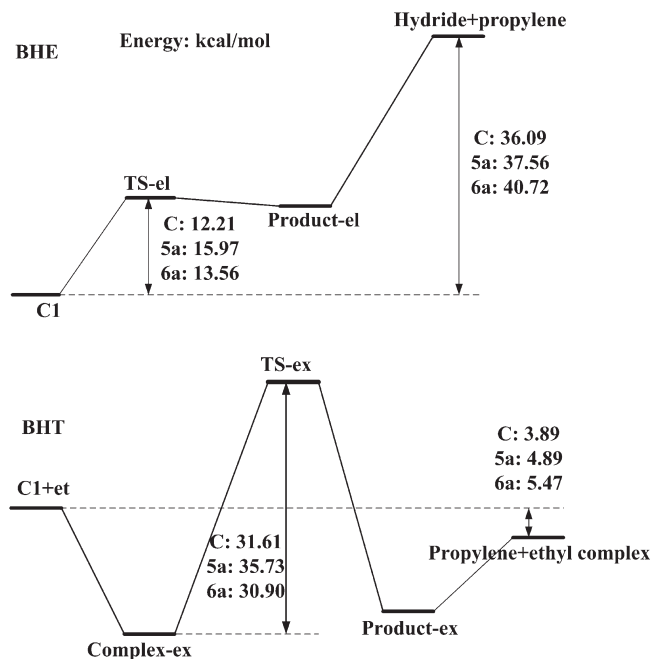


Figure 9. Energy profiles for β-hydride elimination (BHE) and β-hydrogen transfer (BHT) reactions of complexes **C**, **5a**, and **6a**.

reaction coordinates being the distance between the β-carbon of the growing polymer chain and the β-hydride (for the BHE reaction) and the distance between the β-hydrogen of the polymer chain and the carbon of the ethylene molecule (for the BHT reaction). The energy profiles of the BHE and BHT reactions of catalysts **C**, **5a**, and **6a** are shown in Figure 9. As can be seen in the figure, with regard to catalyst **C**, the BHE has a reaction barrier lower than the BHT (12.21 vs 31.61 kcal/mol), but further dissociation of the propylene molecule after BHE reaction is strongly endothermic (36.09 kcal/mol higher than C1). In contrast, the dissociation product after BHT is about 3.89 kcal/mol more stable than the starting isomers (C1+ et). In light of this, the BHT reaction is the feasible chain termination pathway for ethylene polymerization catalyzed by **C**, and similar calculation conclusions were also found for **5a** and **6a**, which is in line with the DFT results reported in the literature.^{20a} Therefore, only the BHT reaction was

(21) (a) Deng, L.; Margl, P.; Ziegler, T. *J. Am. Chem. Soc.* **1997**, *119*, 1094. (b) Deng, L.; Woo, T. K.; Cavallo, L.; Margl, P. M.; Ziegler, T. *J. Am. Chem. Soc.* **1997**, *119*, 6177.

(20) (a) Mary, S. W.; Deng, L. Q.; Ziegler, T. *Organometallics* **2000**, *19*, 2714. (b) Michalak, A.; Ziegler, T. *Organometallics* **2003**, *22*, 2069.

Table 3. DFT Energies (kcal/mol) of π -Complexes, Products, Transition States (TSs), and Reaction Barriers of Ethylene Insertion Reaction and β -Hydrogen Transfer Reaction of **C**, **5a**, and **6a**

reaction	cat.	π -complex	TS	product	energy barrier
ethylene insertion	C	-13.05	1.22	-17.54	14.27
	5a	-16.05	0.35	-18.88	16.40
	6a	-15.80	4.42	-24.85	20.22
β -hydrogen transfer	C	-16.03	15.57	-13.19	31.61
	5a	-18.28	17.45	-12.34	35.73
	6a	-16.10	14.80	-12.62	30.90

compared with the insertion reaction in the ethylene polymerization of catalysts **C**, **5a**, and **6a**.

The DFT energies of π -complexes, products, transition states (TSs), and reaction barriers of the ethylene insertion reaction and the BHT reaction of **C**, **5a**, and **6a** are given in Table 3. Our calculations show that **5a** has reaction barriers higher than **C** in both ethylene insertion and BHT reactions. The great difference in structures should be responsible for this. The phenyl group directed toward the nickel center of complex **5a** can lead to a hindrance not only to the ethylene insertion but also to the BHT. Catalyst **5a** displays a lower chain propagation rate and also a decreased BHT reaction rate relative to those of catalyst **C** in ethylene polymerization. The insertion barrier of catalyst **5a** is about 14.9% more than that of catalyst **C**, while the BHT barrier of **5a** is about 13.0% greater. There is no big difference in the energy increases of both the insertion and BHT reactions for catalysts **5a** compared with **C**. Therefore, the decreased values of the insertion and BHT reaction rates are probably on a similar level. As a result, polyethylenes with molecular weights that are not very different should be produced by catalysts **5a** and **C**, which agrees with the experimental results.

Catalysts **5a** and **6a**, characterized by different catalyst backbones, show very different ethylene insertion and BHT reaction barriers (Table 3), indicating that variation of the ligand types can lead to a great effect on the ethylene polymerization process. Specifically, the reaction barrier of BHT for **6a** (30.90 kcal/mol) is much lower than that of **5a** (35.73 kcal/mol). On the other hand, the reaction barrier of ethylene insertion for **6a** is 3.82 kcal/mol higher than that of **5a**. All the results suggests that catalyst **6a** exhibits a lower chain-propagating rate but a much faster chain termination relative to those of catalyst **5a**. As a result, polyethylenes with much lower molecular weights should be produced by **6a** in comparison with the values for **5a**, which is well consistent with the above experimental results.

Conclusions

A new strategy for modifying stabilities of neutral nickel catalysts for olefin polymerization has been successfully developed by adding a substituent directed toward the metal center. Benefiting from the sterically crowded nickel center, complex **5a** showed an unusual stability under the polymerization conditions and the bis-ligated deactivation has been entirely avoided. The different ethylene polymerization processes of catalysts **C** and **5a** have been directly observed on the basis of ^1H NMR monitoring at room temperature. Complexes **5a** and **7b** exhibited a much stronger tolerance to additional pyridine than their parent complexes **C** and **7a**, respectively. Temperature and ethylene pressure displayed a

greater effect on polymerization behaviors of complex **7b** relative to that of **5a** due to differences in catalyst structure. In addition, the ligand backbone can greatly affect the molecular weight of the polyethylene produced. Polyethylenes with greatly decreased molecular weights were produced by the phenoxyiminato complexes **6a,b** relative to those of the β -ketiminato complexes **5a,b**, which is perfectly consistent with the DFT calculations showing that complex **6a** exhibits a higher ethylene insertion energy but a lower chain termination barrier than those of complex **5a**.

Experimental Section

General Procedures and Materials. All work involving air- and/or moisture-sensitive compounds was carried out under a dry nitrogen atmosphere using standard Schlenk techniques or under a dry argon atmosphere in an MBraun glovebox, unless otherwise noted. All solvents used were purified from an MBraun SPS system. The NMR data of ligands and complexes were obtained on a Bruker 300 MHz spectrometer at ambient temperature with CDCl_3 or C_6D_6 as a solvent. The NMR analyses of polymers were performed on a Varian Unity 400 MHz spectrometer at 135 °C, using *o*- $\text{C}_6\text{D}_4\text{Cl}_2$ as the solvent. The differential scanning calorimetric (DSC) measurements were performed with a PerkinElmer Pyris 1 DSC differential scanning calorimeter at a rate of 10 °C/min. The molecular weights and the polydispersities of the polymer samples were determined at 150 °C by a PL-GPC 220 type high-temperature chromatograph equipped with three PLgel 10 μm Mixed-B LS type columns. 1,2,4-Trichlorobenzene (TCB) was employed as the solvent at a flow rate of 1.0 mL/min. The calibration was made by the polystyrene standard EasiCal PS-1 (PL Ltd.).

1-Tetralone was purchased from Aldrich Chemicals and directly used without purification. 2,6-Diisopropylaniline and methyllithium were obtained from Acros. Potassium *tert*-butoxide was purchased from Aldrich Chemicals. $\text{RuH}_2(\text{CO})(\text{PPh}_3)_3$ and $\text{Py}_2\text{Ni}(\text{CH}_3)_2$ were prepared according to the literature.²² Commercial ethylene was used without further purification.

Synthesis of Substituted 1-Tetralone (compounds **2a,b) (ref 23).** To a 100 mL bottle were added 2.0 mL (14.0 mmol) of 1-tetralone, 3.9 g of phenylboric ester, and 0.7 g of $\text{RuH}_2(\text{CO})(\text{PPh}_3)_3$ as the cocatalyst and 9.0 mL of pinacolone. Subsequently, the bottle was sealed under a N_2 atmosphere and was heated to 140 °C for 2 h. At the end of the reaction, a dark red solution was formed. Finally, 1.4 g (44%) of the product (**2a**) was obtained as a white solid after purification. Compound **2b** was prepared using a similar method with a similar yield (52%).

8-Phenyl-3,4-dihydro-2H-naphthalen-1-one (2a**).** ^1H NMR (300 MHz, CDCl_3): δ 7.43–7.15 (m, 8H, Ar-H), 3.02 (t, 2H, $J = 6.0$ Hz, ArCH₂), 2.62 (t, 2H, $J = 6.6$ Hz, COCH₂), 2.15 (tt, $J = 6.6, 6.0$ Hz, 2H, CH₂). ^{13}C NMR (300 MHz, CDCl_3): δ 198.42 (OC), 145.70, 144.05, 143.06, 131.91, 131.34, 130.37, 128.31, 127.87, 126.68, (Ar), 40.58, 30.81, 23.19, (C). Anal. Calcd for $\text{C}_{16}\text{H}_{14}\text{O}$: C, 86.45; H, 6.35; N, 7.20. Found: C, 86.42; H, 6.37; N, 7.22.

8-Norbornyl-3,4-dihydro-2H-naphthalen-1-one (2b**).** ^1H NMR (300 MHz, CDCl_3): δ 7.37–7.25 (m, 1H, Ar-H), 7.7–7.04 (m, 2H, Ar-H), 3.65 (t, 2H, $J = 6.2$ Hz, ArCH₂), 2.92 (t, 2H, $J = 6.6$ Hz, COCH₂), 2.64 (tt, $J = 6.6, 6.2$ Hz, 2H, CH₂), 2.31 (m, 2H, CH₂), 2.09–1.90 (m, 3H, CH), 1.59–1.21 (m, 6H, CH₂). ^{13}C NMR (300 MHz, CDCl_3): δ 200.47 (OC), 150.52, 146.24, 132.42,

(22) (a) Kakiuchi, F.; Sekine, S.; Tanaka, Y.; Kamatami, A.; Sonoda, M.; Chatani, N.; Murai, S. *Bull. Chem. Soc. Jpn.* **1995**, *68*, 62. (b) Campora, J.; Conejo, M. M.; Mereiter, K.; Palma, P. *J. Organomet. Chem.* **2003**, *683*, 220.

(23) Kakiuchi, F.; Matsuura, Y.; Kan, S.; Chatani, N. *J. Am. Chem. Soc.* **2005**, *127*, 5936.

131.52, 126.58, 125.35, (Ar), 44.54, 43.27, 41.74, 40.20, 37.49, 37.23, 31.72, 30.95, 29.43, 23.30, (C). Anal. Calcd for $C_{17}H_{20}O$: C, 84.96; H, 8.39; N, 6.66. Found: C, 84.98; H, 8.35; N, 6.65.

Synthesis of Ligands 3a,b. To a slurry of 3.3 g of potassium *tert*-butoxide (1.5 equiv) in anhydrous diethyl ether (40 mL) were added 4.4 g of **2a** (20 mmol) and 2.9 g of ethyl formate (2.0 equiv) at 0 °C. Immediately a large amount of white solid appeared in the reaction bottle, and the mixture was stirred for 30 min at 0 °C. Then the resulting suspension was warmed to room temperature and stirred for about 10 h. The white solid was separated by filtration and dried under reduced pressure. Formic acid in ethanol was added to the solid until the pH was < 7, affording the corresponding β -diketone, which was used directly in the preparation of ligand **3a**. Subsequently, 3.5 g of 2,6-diisopropylaniline (1.0 equiv) was added to the obtained β -diketone in ethanol and the condensation reaction was carried out for about 24 h, yielding 4.2 g of ligand **3a** (51%). Ligand **3b** was prepared according to the same method as **3a**.

(2,6- i Pr $_2$ C $_6$ H $_3$)N=CHC $_{16}$ H $_{12}$ OH (3a). 1 H NMR (300 MHz, CDCl $_3$): δ 11.08 (d, $^3J_{\text{HH}} = 12.0$ Hz, 1H, N-H), 7.40–7.11 (m, 11H, Ar-H), 6.72 (d, $J = 12.0$ Hz, 1H, NCH), 3.17 (sept, $^3J_{\text{HH}} = 6.9$ Hz, 2H, i Pr-CH), 2.92 (t, $^3J_{\text{HH}} = 6.6$ Hz, 2H, CH $_2$), 2.59 (t, $^3J_{\text{HH}} = 6.6$ Hz, 2H, CH $_2$), 1.16 (d, $^3J_{\text{HH}} = 6.9$ Hz, 12H, i Pr-CH $_3$). 13 C NMR (300 MHz, CDCl $_3$): δ 188.09 (NC), 150.99, 145.41, 144.08, 143.95, 143.32, 137.30, 134.73, 130.87, 130.71, 129.10, 128.21, 127.82, 127.58, 126.90, 124.10, (Ar), 104.91 (C), 32.05, 28.12, (CH $_2$), 28.78 (i Pr-CH), 24.27 (i Pr-CH $_3$).

(2,6- i Pr $_2$ C $_6$ H $_3$)N=CHC $_{17}$ H $_{18}$ OH (3b). Yield: 61%. 1 H NMR (300 MHz, CDCl $_3$): δ 11.42 (d, $^3J_{\text{HH}} = 12.0$ Hz, 1H, N-H), 7.52–6.98 (m, 6H, Ar-H), 6.74 (d, $J = 12.0$ Hz, 1H, NCH), 3.95 (m, 1H, ArCH), 3.28 (sept, $^3J_{\text{HH}} = 6.9$ Hz, 2H, i Pr-CH), 2.82 (m, 2H, CH $_2$), 2.44 (m, 2H, CH $_2$), 2.35 (m, 1H, CH), 1.97 (m, 1H, CH), 1.63–1.55 (m, 6H, CH $_2$), 1.23 (d, $^3J_{\text{HH}} = 6.9$ Hz, 12H, i Pr-CH $_3$), 0.86 (m, 2H, CH $_2$). 13 C NMR (300 MHz, CDCl $_3$): δ 190.37 (NC), 150.33, 149.37, 144.88, 143.90, 130.67, 127.37, 125.64, 125.43, 124.27, 124.11, (Ar), 105.85 (C), 44.10, 43.40, 40.82, 37.59, 37.27, 32.50, 31.07, 29.52, 28.76, 28.14, 24.33, 24.26, (C).

Synthesis of Ligands 4a,b. To a 100 mL bottle were added 0.4 g of compound **3a** (1 mmol) and 0.24 g of DDQ (1.04 mmol) followed by 5 mL of dioxane, forming a dark mixture. Then the mixture was stirred at the refluxing temperature for 1 h, and a yellow solution formed. The solution was cooled to room temperature, followed by filtration to remove the solid residue. Subsequently, the solvent was evaporated and the product was purified via column chromatography on silica gel, affording 0.2 g (50%) of yellow solid **4a** at room temperature. Ligands **4b** was prepared according to the same method as **4a** with a similar yield.

(2,6- i Pr $_2$ C $_6$ H $_3$)N=CHC $_{16}$ H $_{10}$ OH (4a). 1 H NMR (300 MHz, CDCl $_3$): δ 14.45 (s, 1H, O-H), 8.16 (s, 1H, NCH), 7.75 (dd, $J = 6.0, 0.9$ Hz, 1H, Ar-H), 7.57 (t, $J = 6.0$ Hz, 1H, Ar-H), 7.47–7.34 (m, 6H, Ar-H), 7.29–7.27 (m, 2H, Ar-H), 7.22–7.14 (m, 3H, Ar-H), 2.98 (sept, $^3J_{\text{HH}} = 5.4$ Hz, 2H, i Pr-CH), 1.14 (d, $^3J_{\text{HH}} = 5.4$ Hz, 12H, i Pr-CH $_3$). 13 C NMR (300 MHz, CDCl $_3$): δ 165.00 (NC), 144.91, 142.22, 140.87, 138.31, 130.10, 129.34, 128.83, 128.37, 127.98, 127.40, 126.62, 123.77, 118.26, (Ar), 28.57 (i Pr-CH), 24.06 (i Pr-CH $_3$).

(2,6- i Pr $_2$ C $_6$ H $_3$)N=CHC $_{17}$ H $_{16}$ OH (4b). Yield: 45%. 1 H NMR (300 MHz, CDCl $_3$): δ 8.17 (s, 1H, NCH), 7.53–7.44 (m, 3H, Ar-H), 7.22 (m, 3H, Ar-H), 7.17–7.12 (m, 2H, Ar-H), 4.41 (m, 1H, ArCH), 3.10 (sept, $^3J_{\text{HH}} = 5.4$ Hz, 2H, i Pr-CH), 2.35 (b, 1H, CH), 2.07 (m, 1H, CH), 1.69–1.55 (m, 6H, CH $_2$), 1.22 (d, $^3J_{\text{HH}} = 5.4$ Hz, 12H, i Pr-CH $_3$), 0.86 (m, 2H, CH $_2$). 13 C NMR (300 MHz, CDCl $_3$): δ 169.41 (NC), 165.26, 148.37, 143.61, 140.90, 139.20, 129.17, 127.82, 126.55, 126.27, 123.86, 123.69, 118.84, 112.38, (Ar), 45.84, 43.39, 40.44, 37.83, 37.15, 31.07, 29.72, 28.72, 24.10, 24.04, (C).

Synthesis of Complexes 5a,b, 6a,b, and 7a,b. To [(pyridine) $_2$ -NiMe $_2$] (0.27 g, 1.1 mmol) and the ligand **3a** (1.0 mmol) in a 100 mL septum-capped Schlenk bottle was added toluene (15 mL) at

25 °C. Immediate methane evolution was observed, which ceased within 5–10 min. The resulting red solution was stirred for an additional 4 h at 25 °C, during which time excess [(pyridine) $_2$ -NiMe $_2$] decomposed to nickel black. The resulting mixture was filtrated to remove nickel black, the residue was extracted with toluene, and all volatiles were removed under reduced pressure to yield pure samples of pyridine complex **5a** as a red powder in a high yield (92%). Complexes **5b** and **6a,b** were prepared using the same procedure with similar yields.

[(2,6- i Pr $_2$ C $_6$ H $_3$)N=CHC $_{16}$ H $_{10}$ O]Ni(Me)(Py) (5a). 1 H NMR (300 MHz, C $_6$ D $_6$): δ 7.96 (m, 2H, *o*-H Py), 7.44 (d, $J = 5.4$ Hz, 1H, Ar-H), 7.29 (s, 4H, Ar-H, NCH), 7.25 (s, 1H, Ar-H), 7.18–7.10 (m, 4H, Ar-H), 7.02 (d, $J = 5.1$ Hz, 2H, Ar-H), 6.69 (t, $J = 5.7$ Hz, 1H, *p*-H Py), 6.26 (t, $J = 5.4$ Hz, 2H, *m*-H Py), 4.57 (sept, $^3J_{\text{HH}} = 5.1$ Hz, 2H, i Pr-CH), 2.73 (m, 2H, CH $_2$), 2.49 (m, 2H, CH $_2$), 1.72, 1.41, (d, $^3J_{\text{HH}} = 5.1$ Hz, 12H, i Pr-CH $_3$), –0.62 (s, 3H, NiCH $_3$). 13 C NMR (300 MHz, C $_6$ D $_6$): δ 169.93 (NC), 160.44, 151.96, 151.68, 151.41, 144.37, 142.70, 142.41, 140.71, 134.90, 130.69, 129.43, 127.78, 126.78, 126.23, 125.85, 123.62, 123.24, (Ar, Py), 105.41 (=C), 31.69, 27.25, (CH $_2$), 28.65 (i Pr-CH), 25.35, 23.71, (i Pr-CH $_3$), –6.23 (Ni-CH $_3$). Anal. Calcd for C $_{35}$ H $_{38}$ N $_2$ NiO: C, 74.88; H, 6.82; N, 4.99. Found: C, 74.85; H, 6.79; N, 5.01.

[(2,6- i Pr $_2$ C $_6$ H $_3$)N=CHC $_{17}$ H $_{16}$ O]Ni(Me)(Py) (5b). Yield: 90%. 1 H NMR (300 MHz, C $_6$ D $_6$): δ 8.75 (m, 2H, *o*-H Py), 7.25–6.96 (m, 7H, Ar-H, NCH), 6.70 (m, 1H, *p*-H Py), 6.28 (m, 2H, *m*-H Py), 4.72, 4.49 (sept, $^3J_{\text{HH}} = 6.9$ Hz, 2H, i Pr-CH), 3.43 (m, 1H, ArCH), 2.90–0.94 (m, 14H, CH, CH $_2$), 1.77, 1.68 (d, $^3J_{\text{HH}} = 6.9$ Hz, 6H, i Pr-CH $_3$), 1.36, 1.23 (dd, $^3J_{\text{HH}} = 6.9, 4.2$ Hz, 6H, i Pr-CH $_3$), –0.46 (s, 3H, NiCH $_3$). 13 C NMR (300 MHz, C $_6$ D $_6$): δ 172.21 (NC), 160.79, 152.21, 151.75, 150.06, 144.65, 143.83, 142.85, 142.66, 142.51, 135.89, 130.89, 125.93, 125.44, 124.74, 124.20, 123.62, (Ar, Py), 105.41 (=C), 44.50, 43.97, 43.47, 41.37, 40.99, 40.56, 37.75, 37.35, 36.96, 32.62, 31.33, 30.30, 30.13, 29.64, 28.89, 28.74, 28.61, 28.38, 27.69, 25.35, 25.23, 24.10, 23.74, 23.65, (C), –5.80 (Ni-CH $_3$). Anal. Calcd for C $_{36}$ H $_{42}$ N $_2$ NiO: C, 74.88; H, 7.33; N, 4.85. Found: C, 74.90; H, 7.30; N, 4.88.

[(2,6- i Pr $_2$ C $_6$ H $_3$)N=CHC $_{16}$ H $_{10}$ O]Ni(Me)(Py) (6a). Yield: 94%. 1 H NMR (300 MHz, CDCl $_3$): δ 8.11 (m, 2H, *o*-H Py), 7.71 (s, 1H, NCH), 7.62 (d, $J = 6.0$ Hz, 1H, Ar-H), 7.37 (m, 1H, Ar-H), 7.31 (m, 1H, Ar-H), 7.24–7.05 (m, 6H, Ar-H), 6.88 (t, $J = 5.7$ Hz, 2H, Ar-H), 6.72 (t, $J = 5.7$ Hz, 2H, Ar-H), 6.68 (t, $J = 5.7$ Hz, 1H, *p*-H Py), 6.25 (t, $J = 5.4$ Hz, 2H, *m*-H Py), 4.37 (sept, $^3J_{\text{HH}} = 5.1$ Hz, 2H, i Pr-CH), 1.64, 1.29, (d, $^3J_{\text{HH}} = 5.1$ Hz, 12H, i Pr-CH $_3$), –0.67 (s, 3H, NiCH $_3$). 13 C NMR (300 MHz, C $_6$ D $_6$): δ 167.83 (NC), 164.94, 151.82, 150.74, 145.36, 142.52, 141.65, 139.88, 135.03, 130.74, 129.71, 129.09, 127.03, 126.52, 125.70, 123.81, 123.66, 114.94, 114.60, (Ar, Py), 28.76 (i Pr-CH), 25.17, 23.55, (i Pr-CH $_3$), –5.86 (Ni-CH $_3$). Anal. Calcd for C $_{35}$ H $_{36}$ N $_2$ NiO: C, 75.15; H, 6.49; N, 5.01. Found: C, 75.13; H, 6.52; N, 4.98.

[(2,6- i Pr $_2$ C $_6$ H $_3$)N=CHC $_{17}$ H $_{16}$ O]Ni(Me)(Py) (6b). Yield: 92%. 1 H NMR (300 MHz, CDCl $_3$): δ 8.75 (m, 2H, *o*-H Py), 7.71 (s, 1H, NCH), 7.57 (dd, $J = 5.1, 1.8$ Hz, 1H, Ar-H), 7.46–7.39 (m, 3H, Ar-H), 7.24–7.05 (m, 4H, Ar-H), 6.77 (t, $J = 5.7$ Hz, 1H, *p*-H Py), 6.36 (t, $J = 5.4$ Hz, 2H, *m*-H Py), 4.49, 4.37 (sept, $^3J_{\text{HH}} = 5.1$ Hz, 2H, i Pr-CH), 3.75 (dd, $J = 6.6, 3.9$ Hz, 1H, ArCH), 2.50 (b, 1H, CH), 2.19 (b, 1H, CH), 1.74, 1.63 (d, $^3J_{\text{HH}} = 5.1$ Hz, 6H, i Pr-CH $_3$), 1.59–1.34 (m, 6H, CH $_2$), 1.29, 1.26 (d, $^3J_{\text{HH}} = 5.1$ Hz, 6H, i Pr-CH $_3$), 1.01 (m, 2H, CH $_2$), –0.52 (s, 3H, NiCH $_3$). 13 C NMR (300 MHz, C $_6$ D $_6$): δ 169.69 (NC), 165.35, 152.39, 150.79, 148.40, 141.80, 140.84, 136.04, 130.34, 126.67, 126.53, 123.92, 123.84, 123.71, 122.13, 115.52, 115.17, (Ar, Py), 45.03, 41.52, 40.86, 37.99, 37.29, 30.36, 30.25, 29.90, 28.84, 28.71, 25.20, 25.04, 23.64, 23.50, (C), –5.37 (Ni-CH $_3$). Anal. Calcd for C $_{36}$ H $_{44}$ N $_2$ NiO: C, 74.62; H, 7.65; N, 4.83. Found: C, 74.65; H, 7.67; N, 4.86.

[(2,6- i Pr $_2$ C $_6$ H $_3$)N=CHCHC(C $_6$ H $_4$)O]Ni(Me)(Py) (7a). Yield: 96%. 1 H NMR (300 MHz, CDCl $_3$): δ 8.65 (d, $J = 5.1$ Hz, 2H,

o-H Py), 7.73 (m, 2H, Ar-H), 7.18–7.05 (m, 7H, Ar-H, NCH), 6.59 (t, $J = 7.5$ Hz, 1H, *p*-H Py), 6.21 (t, $J = 6.9$ Hz, 2H, *m*-H Py), 5.86 (d, $J = 6.6$ Hz, 1H, CH), 4.42 (sept, $^3J_{\text{HH}} = 6.9$ Hz, 2H, $^1\text{Pr-CH}$), 1.60, 1.26, (d, $^3J_{\text{HH}} = 6.9$ Hz, 12H, $^1\text{Pr-CH}_3$), -0.55 (s, 3H, NiCH₃). ¹³C NMR (300 MHz, C₆D₆): δ 175.62 (NC), 160.64, 152.11, 144.64, 144.04, 142.52, 140.22, 135.85, 129.89, 129.57, 127.22, 126.90, 126.10, 124.32, 123.63, 123.33, (Ar, Py), 92.53, (=C), 28.58 ($^1\text{Pr-CH}$), 25.31, 23.59, ($^1\text{Pr-CH}_3$), -6.26 (Ni-CH₃). Anal. Calcd for C₂₉H₃₄N₂NiO: C, 70.61; H, 7.02; N, 6.10. Found: C, 70.64; H, 7.06; N, 6.06.

[(2,6-¹Pr₂C₆H₃)N=CHCHC(2'-phenyl-C₆H₄O)]Ni(Me)(Py) (**7b**). Yield: 94%. ¹H NMR (300 MHz, CDCl₃): δ 7.94 (d, $J = 5.7$ Hz, 2H, *o*-H Py), 7.55–7.20 (m, 9H, Ar-H, NCH), 7.08–6.89 (m, 3H, Ar-H), 6.85 (d, $J = 6.3$ Hz, 1H, NCH), 6.53 (t, $J = 7.8$ Hz, 1H, *p*-H Py), 6.12 (t, $J = 6.9$ Hz, 2H, *m*-H Py), 5.40 (d, $J = 6.3$ Hz, 1H, CH), 4.37 (sept, $^3J_{\text{HH}} = 6.9$ Hz, 2H, $^1\text{Pr-CH}$), 1.60, 1.29, (d, $^3J_{\text{HH}} = 6.9$ Hz, 12H, $^1\text{Pr-CH}_3$), -0.70 (s, 3H, NiCH₃). ¹³C NMR (300 MHz, C₆D₆): δ 177.64 (NC), 159.82, 151.97, 143.31, 142.32, 142.12, 135.16, 130.76, 129.49, 128.71, 127.31, 126.99, 125.96, 123.55, 123.08, (Ar, Py), 97.56, (=C), 28.56 ($^1\text{Pr-CH}$), 25.30, 23.60, ($^1\text{Pr-CH}_3$), -6.24 (Ni-CH₃). Anal. Calcd for C₂₉H₃₄N₂NiO: C, 74.04; H, 6.78; N, 5.23. Found: C, 74.06; H, 6.81; N, 5.20.

Synthesis of Bis-ligand Complex of C. To a suspension of NaH (2.0 equiv) in anhydrous THF (10 mL) was added at room temperature 0.13 g of ligand **3a** (0.4 mmol). Immediately a large amount of bubbles was emitted from the mixture and a yellow solution formed. Then the solution was stirred at room temperature overnight and then filtered, affording the sodium salt solution. Subsequently, 61.6 mg (0.2 mmol) of (DME)NiBr₂ was added in the solution with vigorous stirring, and a large amount of white solid appeared, rapidly forming a dark green mixture. After about 4 h, the mixture was filtered to remove the resulting NaBr, and the filtrate was dried in vacuo to afford 0.13 g (90%) of the product as a green solid. ¹H NMR (300 MHz, C₆D₆): δ 7.31 (t, $J = 7.5$ Hz, 2H, Ar-H), 7.22–7.10 (m, 4H, Ar-H), 7.02 (m, 4H, Ar-H), 6.90 (t, $J = 7.2$ Hz, 2H, Ar-H), 6.75 (d, $J = 7.2$ Hz, 2H, Ar-H), 6.54 (s, 2H, N=C-H), 4.85 (sept, $^3J_{\text{HH}} = 6.9$ Hz, 4H, $^1\text{Pr-CH}$), 2.42, 2.11 (t, $J = 7.2$ Hz, 8H, CH₂), 1.40, 1.29 (d, $^3J_{\text{HH}} = 6.9$ Hz, 24H, $^1\text{Pr-CH}_3$). ¹³C NMR (300 MHz, CDCl₃): δ 165.15 (NC), 159.30, 146.88, 142.30, 137.82, 131.08, 128.02, 125.55, 125.20, 124.72, 124.11, 122.66, (Ar), 101.55, (=C), 28.14, 27.66 ($^1\text{Pr-CH}$), 24.46, 23.43, 22.50 ($^1\text{Pr-CH}_3$). Anal. Calcd for C₄₆H₅₂N₂NiO₂: C, 76.35; H, 7.24; N, 3.87. Found: C, 76.32; H, 7.26; N, 3.85.

Ethylene Polymerization. A 200 mL autoclave was heated under vacuum to 130 °C for 10 h and then was cooled to the desired reaction temperature in an oil bath with constant temperature. The vessel was purged three times with ethylene and then was charged with toluene (50 mL) under vacuum. A 10 or 20 μmol amount of cocatalyst dissolved in 10 mL of toluene was added into the autoclave by syringe if necessary, followed by the same amount of catalyst. The total volume of the reaction medium was fixed at 100 mL. Then the reactor was sealed and pressurized to the desired level, and the stirring motor was engaged. Temperature control was maintained by internal cooling water coils with temperature increases within 2 °C in every case. After the prescribed reaction time, the stirring motor was stopped, the reactor was vented, and the polymer was isolated

via precipitation from ethanol. The solid polyethylene was filtered, washed with acetone several times, and dried at 60 °C for more than 10 h under vacuum.

Crystallographic Studies. Crystals for X-ray analysis were obtained as described in the preparations. The crystallographic data, collection parameters, and refinement parameters are given in Table 1. The crystals were manipulated in a glovebox. The intensity data were collected with the ω scan mode (186 K) on a Bruker Smart APEX diffractometer with CCD detector using Mo K α radiation ($\lambda = 0.71073$ Å). Lorentz, polarization factors were made for the intensity data, and absorption corrections were performed using the SADABS program. The crystal structures were solved using the SHELXTL program and refined using full-matrix least-squares. The positions of hydrogen atoms were calculated theoretically and included in the final cycles of refinement in a riding mode along with attached carbons.

DFT Studies. We employed density functional theory (DFT) calculations for ethylene insertion and chain termination mechanisms of complexes **C**, **5a**, and **6a** by using the Amsterdam Density Functional (ADF) program package.²⁴ The structures and energies are obtained on the basis of the local density approximation augmented with Becke's nonlocal exchange corrections²⁵ and Perdew's nonlocal correlation correction.²⁶ A triple STO basis set was employed for Ni, while all other atoms were described by a double- ζ plus polarization STO basis. The 1s electrons of the C, N, and O atoms, as well as the 1s–2p electrons of the Ni atom, were treated as frozen core. Finally, first-order scalar relativistic corrections were added to the total energy of the system. DFT calculations were combined with molecular mechanics calculations by using the quantum mechanics/molecular mechanics (QM/MM) implementation in the ADF program.²⁷ Isopropyl groups were represented by a augmented Sybyl force field,²⁸ which includes van der Waals parameters from the UFF force field²⁹ for nickel.

Acknowledgment. We are grateful for the subsidy provided by the National Natural Science Foundation of China (Nos. 20734002 and 20923003).

Supporting Information Available: X-ray diffraction data for **5a** and **6b** (as CIF), the data collection and refinement data of the analysis, necessary ¹H NMR data, and coordinates of DFT-optimized structures. This material is available free of charge via the Internet at <http://pubs.acs.org>.

(24) (a) Baerends, E. J.; Ellis, D. E.; Ros, P. *Chem. Phys.* **1973**, *2*, 41. (b) Baerends, E. J.; Ros, P. *Chem. Phys.* **1973**, *2*, 52. (c) te Velde, G.; Baerends, E. J. *J. Comput. Phys.* **1992**, *99*, 8498. (d) Fonseca, C. G.; Visser, O.; Snijders, J. G.; te Velde, G.; Baerends, E. J. In *Methods and Techniques in Computational Chemistry, METECC-95*; Clementi, E., Corongiu, G., Eds.; STEF: Cagliari, Italy, 1995; p 305.

(25) Becke, A. D. *Phys. Rev. A* **1988**, *38*, 3098.

(26) Perdew, J. P. *Phys. Rev. B* **1986**, *33*, 8822.

(27) Woo, T. K.; Cavallo, L.; Ziegler, T. *Theor. Chem. Acc.* **1998**, *100*, 307.

(28) Clark, M.; Cramer, R. D., III; van Opdenbosch, N. *J. Comput. Chem.* **1989**, *10*, 982.

(29) Rappe, A. K.; Casewit, C. J.; Colwell, K. S.; Goddard, W. A., III.; Skiff, W. M. *J. Am. Chem. Soc.* **1992**, *114*, 10024.